Diminished Electron Cloud Broadening in a Silicon Drift Detector by Sawtooth p^+ Strips

Jan Šonský, Hein Valk, Cédric P. Allier, Rob W. Hollander, *Member, IEEE*,
Carel W. E. van Eijk, *Member, IEEE*, and Pasqualina M. Sarro

***Abstract*— Already in 1993, sawtooth-shaped p^+ strips were proposed to diminish lateral diffusion in linear multi-anode silicon drift detectors. The sawtooth structure generates small electric fields directed parallel to the detector surface and perpendicular to the drift direction. These fields confine the drifting electrons within a sawtooth period. In this paper the authors present for the first time experimental proof of the applicability of the concept. For a sawtooth period of 500 μm, we have tested the confinement of electron clouds as a function of injected charge up to 5 × 10^6 electrons. The maximum number of electrons for which full confinement is achieved has been measured as a function of the potential gutter depth generated by different sawtooth angles.**

***Index Terms*— Charge sharing, electron cloud confinement, multi-anode linear drift detectors.**

I. Introduction

The MULTI-ANODE linear silicon drift detector (SDD) allows us to obtain two-dimensional (2-D) position information [1], [2]. In one direction, the drift direction, position information is obtained from electron drift time measurement. In the lateral direction anode pixel signals are used for position measurement by means of interpolation, or the anode with the highest signal is simply used. In these cases the spatial resolution is determined by the anode pitch and electron cloud broadening. The broadening is generally caused by thermal diffusion and mutual electrostatic repulsion, which take place during the electron drift toward the anode pixels. In the case of a relatively small anode pitch in combination with a small amount of generated charge (<1000 electrons), the cloud broadening becomes a problem. The small signals at the anodes do not allow us to determine the lateral position accurately using interpolation. Another disadvantage of lateral broadening is deterioration of energy resolution. Supposing generation of electrons by incident X-rays in front of the middle of an anode at a distance of 1.25 cm, the electron cloud arriving at the anode pixel after 2.8 μs (at a drift field of 300 V/cm) will have an rms lateral width of 140 μm. In the case of a linear SDD with an anode pitch of 250 μm, only about 63% of these electrons will then be collected at the central anode.

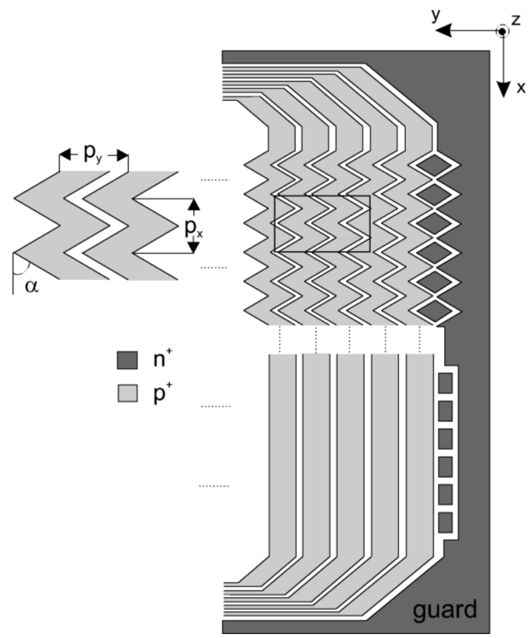

Fig. 1. Schematic of fabricated SDD's with two sections showing sawtooth strips ($\alpha = 60°$) and rectangular ($\alpha = 0°$) strips. The definitions of sawtooth period p_x, pitch p_y, and angle α are shown in detail. The rectangle indicates the simulated region.

Collection of the full charge at one or at most two anodes is preferred to achieve good energy resolution. This requires a new SDD design.

In 1993, Hijzen *et al.* [3] proposed a new drift detector design in which lateral diffusion is diminished by only an appropriate change of the layout of the p^+ field strips, the sawtooth concept. An effort to demonstrate the validity of the concept shortly after its introduction failed by then-occurring problems with the SDD's [4]. In 1996 Castoldi *et al.* [5] demonstrated the applicability of another approach, the deep p-implant "channel-stop" concept. They reported confinement up to 32 000 electrons within an anode pitch of 60 μm. The channel-stop concept requires additional process steps. In the sawtooth concept only the masks are different from those of the standard SDD process and additional process steps are not required.

Without any basic modification of the standard fabrication process, confinement can be realized. In this paper positive results of measurements on new SDD's are presented. We used SDD's with a large anode pitch of 500 μm and charges up to 5.0 × 10^6 electrons. The main purpose is to confirm the

Manuscript received May 19, 1998; revised August 24, 1998. This work was supported by The Netherlands Technology Foundation (STW).

J. Šonský, H. Valk, C. P. Allier, R. W. Hollander, and C. W. E. van Eijk are with the Radiation Technology Group, Interfaculty Reactor Institute, Delft University of Technology, 2629 JB Delft, The Netherlands.

P. M. Sarro is with the Delft Institute of Microelectronics and Submicron Technology, Delft University of Technology, 2628 CD Delft, The Netherlands.

Publisher Item Identifier S 0018-9499(99)02199-1.

theoretical expectation by experimental results which allows us to predict the result for SDD's with an anode pitch of 250 μm, which is sufficient for anticipated soft X-ray diffraction applications.

II. Detector Design and Simulation

In Fig. 1, part of the layout of the studied SDD's is presented. The definitions of the three important parameters of the sawtooth, the period p_x, pitch p_y, and angle α, are also indicated. The detectors have a total active area of 2.5 $\times$ 1.3 cm^2, subdivided into two halves of 1.25 $\times$ 1.3 cm^2 with anodes at the opposite outsides. Each half is divided into two sections (see Fig. 1). The four sections have the following α: 0° (rectangular strips), 30°, 45°, and 60°. Strips have been designed on both front and back sides for appropriate biasing. The back side can be illuminated with a laser beam because the strips are not covered with aluminum. There are only narrow (15 μm) metallization strips overlapping the edges of the p$^+$ strips to improve the breakdown properties.

We used 2–10 kΩ cm n-type wafers of 500-μm thickness. The pitch of p$^+$ strips $p_y = 200$ μm (180 μm p$^+$ implant, 20 μm oxide). The period $p_x = 500$ μm, while the n$^+$ anodes are 400-μm wide. The anodes are insulated with a p$^+$ implantation to avoid a leak of charge to adjacent anodes caused by the small inter-anode resistance. The surrounding n$^+$ guard collects the electrons generated outside the sensor active area. To avoid problems at high drift fields, the guard area is designed in such a way that every p$^+$ field strip is attached to a guard strip. The oxide width between guard strips is the same as between field strips.

To simulate the influence of sawtooth strips on the potential distribution in the detector, we have used the SEMISIM package [3]. This package calculates the quasi-static potential distribution by solving only the Poisson equation using the finite difference algorithm. The simulation shows that the sawtooth-shaped p$^+$ strips generate a confining potential in the x-direction. This effect propagates from the surface down to the center of the wafer [see Fig. 2(a) for $z = 250$ μm]. The depth of these potential gutters depends on the three sawtooth design parameters p_x, p_y, and α, and on the potential distribution applied to the p$^+$ sawtooth strips. The influence of the sawtooth parameters was extensively discussed in [3]. To highlight general design aspects we will comment here only on the important conclusions. As for the sawtooth parameters, the depth of potential gutters increases with increasing sawtooth period p_x and angle α. On the contrary, the pitch p_y influences mainly the effect of the sawtooth in the middle of the strips. To induce the confining effect in the middle of a strip as well, the pitch p_y has to be chosen small enough compared with the period p_x. As one can expect period p_x especially is of great importance. This parameter is equal to the anode pitch and therefore directly linked to the position resolution of the SDD. Thus by designing a sawtooth SDD with a given resolution in the lateral direction, p_x is fixed. Next the sawtooth angle α and pitch p_y have to be properly chosen to obtain potential gutters deep enough for confinement of a desired electron capacity. The depth of generated gutters is also linearly proportional to

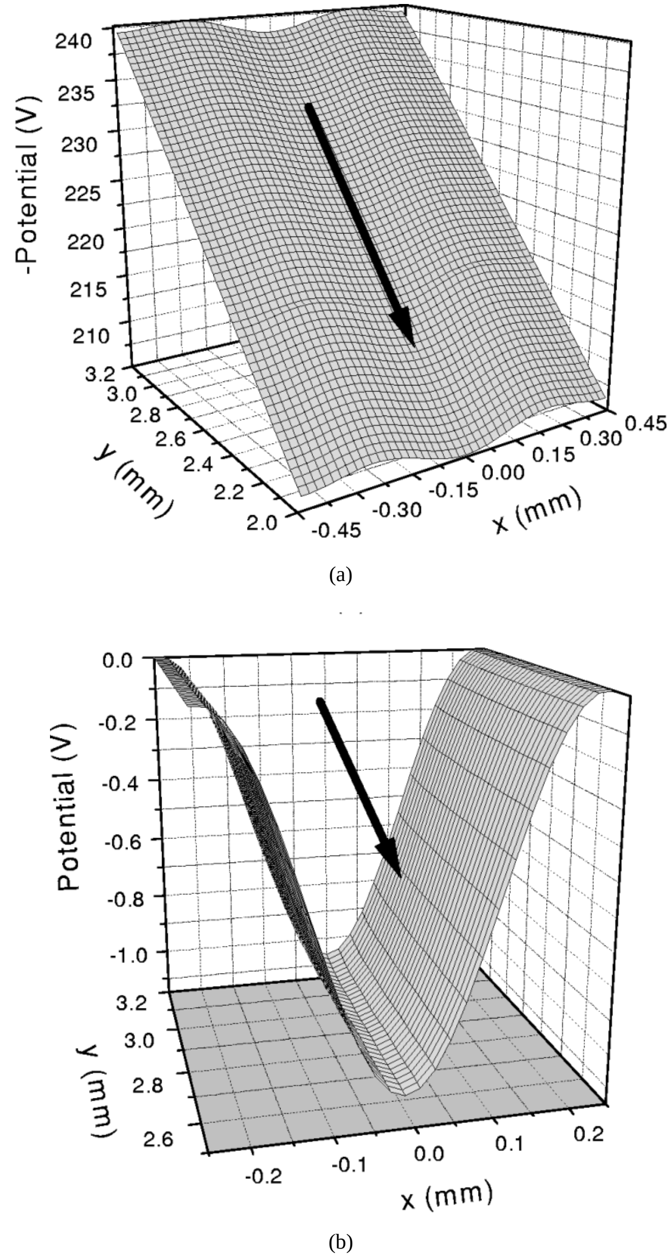

Fig. 2. (a) Potential distribution of the rectangular region indicated in Fig. 1. (b) Potential difference between sawtooth and rectangular strip configuration at a depth in the z-direction corresponding to the potential minimum. The sawtooth parameters are $p_x = 500$ μm, $p_y = 200$ μm, and $\alpha = 60°$. The drift field is 250 V/cm. The arrows indicate the drift direction for electrons.

the potential difference applied between adjacent sawtooth p$^+$ strips, i.e., to the drift field. To obtain the required confining effect the suitable drift field has to be applied.

All simulations of designed sawtooth SDD's have been done using a drift field of 250 V/cm corresponding to the measurement conditions. The potential minimum in the z-direction is located in the center of the wafer ($z = 250$ μm). Fig. 2(a) shows the potential distribution in the SDD of the rectangular area indicated in Fig. 1 ($p_x = 500$ μm, $p_y = 200$ μm, and $\alpha = 60°$) at the depth of the potential minimum for electrons ($z = 250$ μm). One can see the potential gutter (marked by an arrow) through which the electrons will travel toward the anode. To clearly see the depth and the profile of

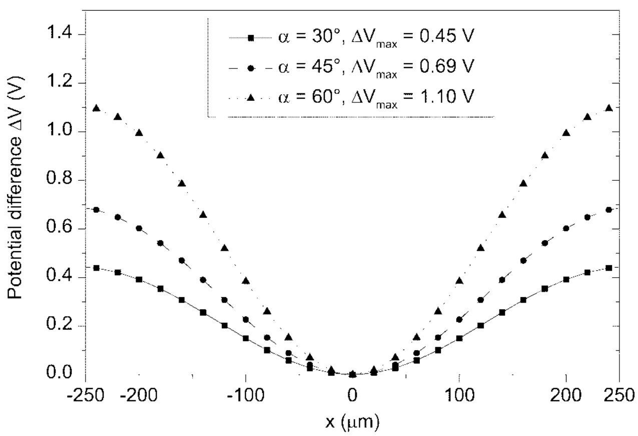

Fig. 3. The influence of the sawtooth angle α on the potential in the gutter. The maximal gutter depth $(\Delta V_{\max})$ is indicated for each angle α. The other parameters are $p_x = 500$ μm, $p_y = 200$ μm, and the drift field is 250 V/cm.

the confining potential, we have subtracted the corresponding potential distribution of the rectangular strip configuration. The resulting potential gutter is plotted in Fig. 2(b). At the bottom of the potential gutter there is a small modulation along the drift direction which, however, does not exceed a few percent of the maximal depth of the gutter.

The influence of the magnitude of α on the depth of the potential gutter is shown in Fig. 3. Plotted again is the potential difference caused by the sawtooth strips. The potential gutter becomes deeper as we increase the angle α.

To estimate the number of electrons which can be confined within a potential gutter, we have to distinguish two situations. For small charge levels ($Q < 10\,000$ el.) only diffusion broadens the electron cloud and a lateral potential barrier as small as a few thermal voltages ($\phi_T = 0.025$ V at room temperature) is sufficient. When we increase the number of injected electrons, the mutual electrostatic repulsion becomes prevailing. The average repulsion energy per electron eV_{rep} for N electrons uniformly distributed inside a sphere of radius R is expressed by [6]

$$V_{\text{rep}} = \frac{e}{4\pi\varepsilon}\,\frac{3}{5}\,\frac{N}{R} \tag{1}$$

where e is the elementary charge and ε the dielectric constant. To the first approximation we can estimate the number of electrons N that can be confined as follows. We assume that the charge cloud of given width is initially positioned in the center of the gutter. The repulsion energy will spread the charge cloud until the lateral barrier of the confining gutter compensates repulsion. Once in equilibrium, the electrons will travel to the anodes without additional broadening.

Assuming that the electron cloud has a Boltzmann-like energy distribution, with an average electron energy equal to $(\phi_T + V_{\text{rep}})$, the condition

$$(\phi_T + V_{\text{rep}}) \leq \tfrac{1}{3}\Delta V_{\max} \tag{2}$$

is necessary for sufficient confinement of N electrons [6]. From (1) and (2) with $R = p_x/2 = 250$ μm and $\Delta V_{\max}$ as indicated in Fig. 3, the number of confined electrons can be obtained. We have calculated that $N = 4.1 \times 10^5$, 6.7×10^5, and 1.1×10^6 electrons for $\alpha = 30$, 45, and $60°$, respectively.

III. Experiment

The SDD's were tested using a pulsed laser beam. Special attention has to be given to the biasing of the sensor. We have applied on the front-side strips a negative potential which is increasing in uniform steps from the first strip (closest to the anode) to the outermost strip. The negative voltage applied on the backside strips has a "V"-shaped potential distribution close to the anodes. This shifts the potential minimum close to the anodes in the z-direction and provides a more effective charge collection, but it does not influence the depth of the potential gutter [3]. The applied drift field was 250 V/cm. We have measured a maximal electron drift time of 4.5 μs for a drift distance of 1.25 cm.

A pulsed laser source (675 nm) has been used to generate signal electrons in the detector. The laser intensity was adjusted using pinholes and filters to generate from 1.7×10^3 to 5×10^6 electrons per pulse. The laser spot has a Gaussian distribution with standard deviation $\sigma = 60$ μm for the smaller charge levels ($Q \leq 4.2 \times 10^5$), and $\sigma = 90$ μm for the higher charge levels ($Q > 4.2 \times 10^5$).

Information on the electron cloud broadening is obtained by measuring the charge collected at an anode for different x-position of the laser spot and at different distances (y-position) from the anode. The measurements have been repeated for several anodes. The results reproduced well. Fig. 4 shows the charge collection over the active area of one anode $(\alpha = 60°)$ for 3.0×10^4 electrons. We can see that the charge collection is uniform along the whole drift length and the lateral profile remains unchanged. This implies that the electron broadening is well controlled.

The measurements have been done for all four sections, with $\alpha = 0, 30, 45$, and $60°$. Fig. 5 shows the cross sections of charge collection after 4 μs of drift time (corresponding to $y = 11$ mm) for $\alpha = 0, 30, 45$, and $60°$. We have used a charge level of 3×10^4 electrons. The injected charge is well confined within one sawtooth period for angles of 30, 45, and 60°. The top of the measured profiles is not well uniform due to the narrow metallization strips overlapping the edges of the p^+ strips. Part of the laser spot is reflected and the number of generated electrons changes. Without saw teeth $(\alpha = 0°)$ we see broadening of the measured profile due to the free diffusion and an extra broadening caused by mutual electrostatic repulsion.

A relatively smooth profile of the confining potential near the edges of the gutter (see Fig. 3) can imply that an electron cloud generated in this region could be shared between two adjacent gutters. To highlight the charge-sharing between two adjacent anodes, we have plotted charge collection profiles at two adjacent anodes in Fig. 6. Fitting the experimental points by a convolution of a Gaussian and the rectangular function of the anode, we can determine the laser spot size. The thus obtained σ of the laser spot matches the value measured by other methods rather well. This allows us to conclude that for $Q = 3 \times 10^4$ electrons charge sharing near the edges is essentially only caused by the finite size of the laser spot. A small extra broadening near the edges is observed for charge levels $Q > 1 \times 10^5$ electrons. This effect is due to the initial

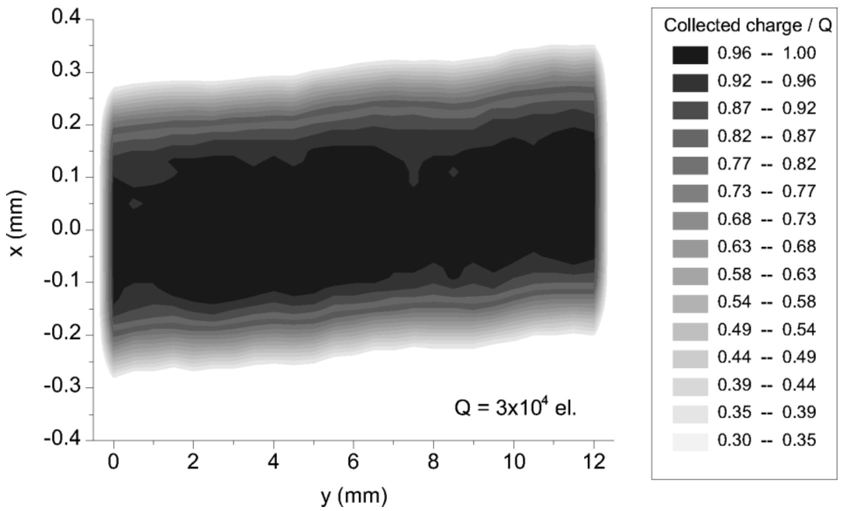

Fig. 4. Normalized charge collection over the whole active area of one anode for $\alpha = 60°$. The center of the anode is located at position (0, 0). We have injected 3.0 $\times$ 10^4 electrons. The profile is not symmetric in x-coordinate due to a small misalignment of laser spot motion and detector.

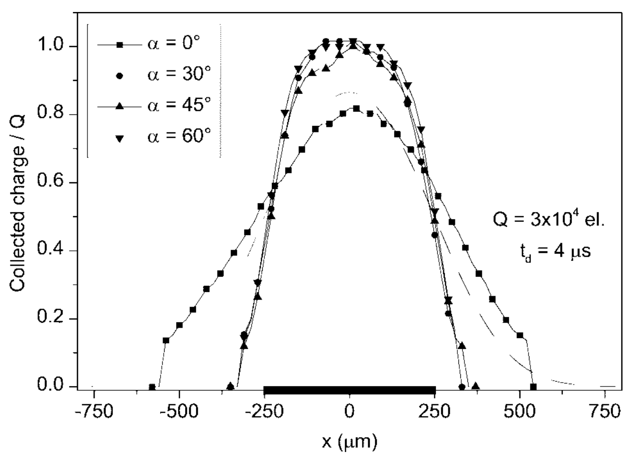

Fig. 5. Normalized charge collection at one anode as a function of x-position of injection after 4 μs of drift time for $\alpha = 0, 30, 45,$ and $60°$. The dashed line shows the calculated profile in the case of thermal diffusion (without electrostatic repulsion). The thicker line on the horizontal axis represents the width of the potential gutter.

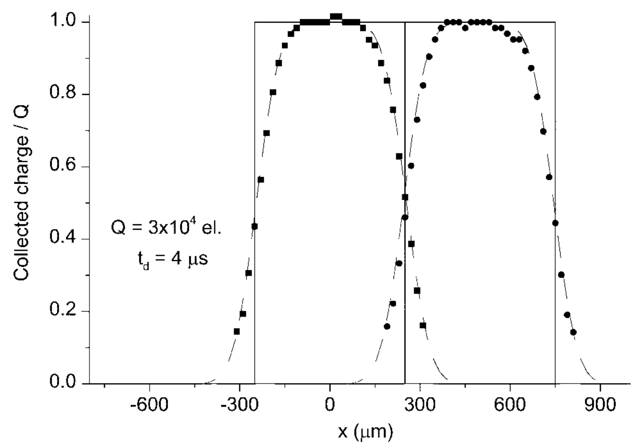

Fig. 6. Normalized charge collection at two adjacent anodes as a function of x-position of injection after 4 μs of drift time for $\alpha = 60°$. The dashed lines show fits of the experimental points by a curve obtained by convolution of the Gaussian laser pulse intensity and the rectangular function of an anode (solid line).

repulsion which is not fully compensated near the edges of the gutter.

Because the estimated maximum of confined electrons is much higher than 3 $\times$ 10^4 electrons, we have performed measurements for electron injection up to 5 $\times$ 10^6 electrons. Fig. 7(a)–(d) shows the set of charge collection profiles at one anode as a function of the lateral position for the following charge levels: 4.2 $\times$ 10^5, 7.75 $\times$ 10^5, 2.5 $\times$ 10^6, and 5.0 $\times$ 10^6 electrons. We have focused our attention on the sensor sections with $\alpha = 30$ and $60°$, because the estimated maxima differ significantly for these two cases. From the charge collection for $\alpha = 30°$ shown in Fig. 7, we can see that the potential gutter is able to confine maximally 4.2 $\times$ 10^5 electrons. When we increased the charge level, the electrons start to fill the next neighboring gutters. Further increasing of the charge level ($Q = 2.5 \times 10^6$ electrons) leads to spreading of injected electrons also to the second neighboring gutters, i.e., injected electrons are confined within five sawtooth periods. It must be noted, however, that the second neighboring gutters remain almost empty. For $\alpha = 60°$, a charge level of 7.75 $\times$ 10^5 electrons was found to be the maximal one which still allows confinement within one gutter, provided that charge injection occurs at the center of the gutter. Off-center charge injection suffers from some overflow. Another increase of the number of charges causes also overflow from the gutter center into adjacent gutters. Nevertheless, all injected electrons are still confined within the central and both next-neighboring gutters, up to 5.0 $\times$ 10^6 electrons. For $\alpha = 0°$, the electron cloud is very strongly widened over many anodes by the mutual repulsion which dominates over the lateral diffusion.

Because the injected charge was varied with large steps, the experimental maximum of confined electrons cannot be found more accurately than at the lower side of the range 4.2–6.2 $\times$ 10^5 electrons for $\alpha = 30°$, and in the range 7.75 $\times$ 10^5–2.5 $\times$ 10^6 electrons for $\alpha = 60°$. The theoretical estimates are located at lower sides of these intervals for both 30 and 60° angles. Therefore, assuming that our theoretical model is accurate enough, we can approximately calculate the

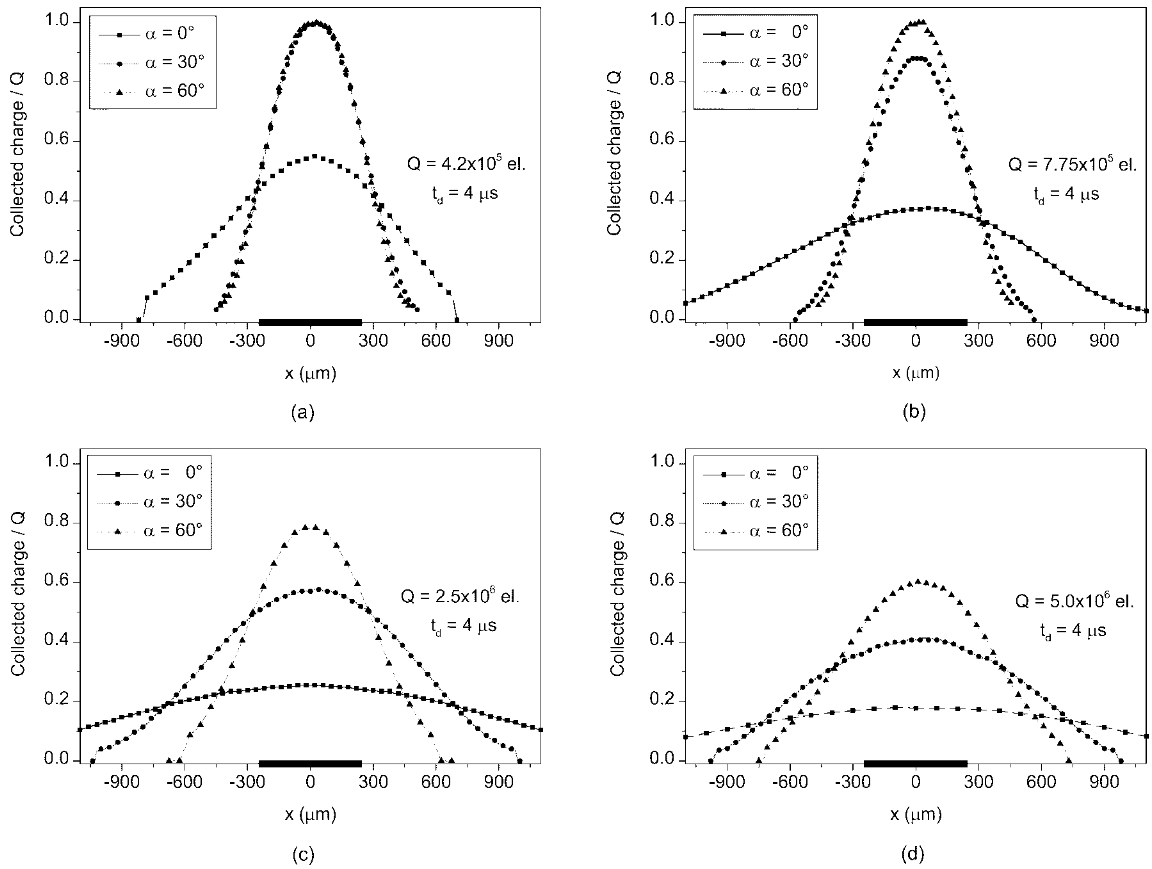

Fig. 7. Comparison of normalized charge collection at one anode as a function of x-position of injection at $y = 11$ mm, i.e., 4 μs of drift time, for $\alpha = 0, 30,$ and 60° for different injected charge levels: (a) $Q = 4.2 \times 10^5$ electrons, (b) $Q = 7.75 \times 10^5$ electrons, (c) $Q = 2.5 \times 10^6$ electrons, and (d) $Q = 5.0 \times 10^6$ electrons. The thicker line on the horizontal axis represents the sawtooth period.

number of confined electrons for $p_x = 250$ μm. Performing the calculation under the same working conditions, the maximal depth of the potential gutter is 0.080 V for $\alpha = 60°$. Such a potential barrier should be able to confine up to about 2.7 $\times$ 10^3 electrons which would be produced by a photon of ~10 keV stopping in the detector.

IV. Discussion and Conclusion

The electron confinement has been tested for laser-light generated electrons, i.e., electrons generated at a depth of $z < 10$ μm. At this depth the confining potential is much deeper than at the center of the wafer and one might be tempted to think that the experiment with laser light is a rather favorable case. However, though the light is absorbed near the surface the confining conditions are determined by the sawtooth potential in the center of the wafer. For clarification we will analyze, by means of single-electron simulation, the time scale of the following processes: the motion of electrons: 1) from the detector surface to the drift potential minimum ($z = 250$ μm); 2) from the edges of the gutter to the center of the gutter; and 3) in electron cloud broadening. Assuming the working conditions used above, the electrons need less than 10 ns to travel from the surface to the drift potential minimum, whereas it takes about 100 ns to travel from the edge of the sawtooth gutter to its center at $z = 10$ μm and even much longer, about 500 ns, at $z = 250$ μm. During the time of 10 ns, a Gaussian-shaped cloud of 7.75 $\times$ 10^5 electrons broadens from $\sigma = 40$ μm to $\sigma = 57$ μm due to the uncompensated electrostatic repulsion [7]. This means that there is only a small cloud broadening and hardly any motion of electrons in the x-direction toward or away from the center of the gutter during the traveling of electrons from the detector surface to the drift potential minimum. Therefore, essentially only the potential gutter at $z = 250$ μm determines the electron cloud broadening. Consequently, the laser-light generated electron cloud experiments are sufficient proof for confinement. This allows us to expect that the sawtooth gutters will also work for other types of radiation-generating electrons deeper in the sensor (such as X rays).

Measurements have been done with charge levels ranging from 1.5 $\times$ 10^3 to 5.0 $\times$ 10^6 electrons. The confining effect is clearly observed, both at small charge levels where electron broadening is mainly caused by thermal diffusion, and at high charge levels where electrostatic repulsion is dominant. At a charge level of 5.0 $\times$ 10^6 electrons, the charge collection profile for $\alpha = 0°$ is strongly broadened over many anodes, while in the cases of $\alpha = 30$ and 60° all injected electrons are distributed over five and three potential gutters, respectively. We have experimentally confirmed the maximum confinement charge levels for $\alpha = 30$ and 60° which have been estimated using an electrostatic model.

Due to the agreement between simulations and experimental measurements we estimate confinement of about 2.7 $\times$ 10^3 electrons for a sawtooth SDD with an anode pitch of 250 μm and $\alpha = 60°$. If necessary, deeper potential gutters allowing confinement of larger electron capacity can be realized by increasing the potential difference between adjacent strips or by drifting closer to the surface of the wafer. Larger values of $\Delta V_{\max}$ can be also achieved by enlarging the sawtooth angle α. However, high electric fields, which are generated around sharp edges of strips with very large angles, may cause a breakdown. It should be noticed that the depth of the potential gutters in the center of the wafer is also dependent on the bulk resistivity and the thickness of the wafer.

We have reported electron confinement in SDD's by means of sawtooth-shaped p^+ strips. This is an alternative way compared to the "channel-stop" concept. Confining potentials generated by properly designed sawtooth strips propagate through the whole thickness of the wafer, i.e., the electron cloud will be confined immediately after generation at any depth of the detector. Traditional biasing schemes sweeping signal electrons to the drifting-potential minimum located in the middle of the detector can be used. On the contrary deep p^+-implants employed in the "channel-stop" concept create confining barriers essentially only inside a thin epitaxial layer. To achieve confinement the electrons have to travel near the interface between bulk and epilayer, and the electron motion might be significantly affected by surface nonlinearity. Moreover, the initial repulsion and diffusion can spread the electron cloud generated in the bulk before reaching the drifting-potential minimum. The main disadvantage of the sawtooth concept is the dependence of $\Delta V_{\max}$ on the period p_x (=anode pitch). We expect that p_x ~200 μm is the smallest value allowing confinement of a small number of electrons. Further decrease of p_x would result in negligible confining effects. Thus the sawtooth concept cannot achieve as good a position resolution as reported for the "channel-stop" concept [5]. The sawtooth concept is mainly intended to eliminate deterioration of energy resolution due to the lateral broadening. An energy resolution comparable with that of a circular SDD, having one central anode, can then be achieved with a multi-anode sawtooth SDD.

REFERENCES

[1] E. Gatti and P. Rehak, "Semiconductor drift chamber—An application of a novel charge transport schema," *Nucl. Instrum. Methods,* vol. A225, pp. 608–614, 1984.

[2] T. J. Summer, G. K. Rochester, G. Hall, S. Roe, R. Wheadon, C. C. Zammit, L. Evensen, and B. S. Avset, "Development of silicon drift chambers for X-ray astronomy," *SPIE, X-Ray and Gamma Ray Instrum. Astronomy and Atomic Phys.,* vol. 1159 EUV, pp. 595–604, 1989.

[3] E. A. Hijzen, E. M. Schooneveld, C. W. E. van Eijk, and R. W. Hollander, "New silicon drift detector design for diminishing lateral diffusion," *Nucl. Instrum. Methods,* vol. A335, pp. 271–275, 1993.

[4] E. A. Hijzen, E. M. Schooneveld, C. W. E. van Eijk, R. W. Hollander, P. M. Sarro, and A. van den Bogaard, "Results of a new silicon drift detector design for diminishing lateral diffusion," in *IEEE Nucl. Sci. Symp. Conf. Rec.,* 1995, pp. 675–678.

[5] A. Castoldi, P. Rehak, and P. Holl, "A new silicon drift detector with reduced lateral diffusion," *Nucl. Instrum. Methods,* vol. A377, pp. 375–380, 1996.

[6] A. Castoldi, P. Rehak, and L. Strüder, "Electron confinement in drift detectors by means of 'channel-stop' implants: Characterization at high signal charges," *IEEE Trans. Nucl. Sci.,* vol. 43, pp. 3201–3206, 1996.

[7] E. Gatti, A. Longoni, P. Rehak, and M. Sampietro, "Dynamics of electrons in drift detectors," *Nucl. Instrum. Methods,* vol. A253, pp. 393–399, 1987.